

Accurate reconstruction of the thermal conductivity depth profile in case hardened steel

Ricardo Celorrio,¹ Estibaliz Apiñaniz,² Arantza Mendioroz,² Agustín Salazar,^{2,a)} and Andreas Mandelis³

¹*Departamento de Matemática Aplicada, EUITIZ/IUMA, Universidad de Zaragoza, Campus Río Ebro, Edificio Torres Quevedo, 50018 Zaragoza, Spain*

²*Departamento de Física Aplicada I, Escuela Técnica Superior de Ingeniería, Universidad del País Vasco, Alameda Urquijo s/n, 48013 Bilbao, Spain*

³*Department of Mechanical and Industrial Engineering, Center for Advanced Diffusion-Wave Technologies, University of Toronto, Toronto, Ontario M5S 3G8, Canada*

(Received 17 December 2009; accepted 9 February 2010; published online 29 April 2010)

The problem of retrieving a nonhomogeneous thermal conductivity profile from photothermal radiometry data is addressed from the perspective of a stabilized least square fitting algorithm. We have implemented an inversion method with several improvements: (a) a renormalization of the experimental data which removes not only the instrumental factor, but the constants affecting the amplitude and the phase as well, (b) the introduction of a frequency weighting factor in order to balance the contribution of high and low frequencies in the inversion algorithm, (c) the simultaneous fitting of amplitude and phase data, balanced according to their experimental noises, (d) a modified Tikhonov regularization procedure has been introduced to stabilize the inversion, and (e) the Morozov discrepancy principle has been used to stop the iterative process automatically, according to the experimental noise, to avoid “overfitting” of the experimental data. We have tested this improved method by fitting theoretical data generated from a known conductivity profile. Finally, we have applied our method to real data obtained in a hardened stainless steel plate. The reconstructed in-depth thermal conductivity profile exhibits low dispersion, even at the deepest locations, and is in good anticorrelation with the hardness indentation test. © 2010 American Institute of Physics. [doi:10.1063/1.3357378]

I. INTRODUCTION

Modulated photothermal radiometry is a well established tool for the thermophysical characterization and the nondestructive evaluation of a wide variety of materials. Since the pioneering work of Mandelis and co-workers,¹ it has been applied to reconstruct the thermal conductivity depth profile of case hardened steel pieces from surface temperature data.² This inverse problem is ill-posed in Hadamard sense, i.e., there is not a continuous relationship between errors in the data and in the thermal conductivity. This means that the same surface temperature is obtained from quite different thermal conductivity profiles (within experimental uncertainty). That is the reason why the reconstructed conductivity is extremely sensitive to noise. However, the ill-posedness of the problem can be attenuated by reducing the number of unknowns. One possibility is to define the shape of the thermal conductivity by a simple function with few parameters.^{3–6} The second possibility is to use a multilayered model to simulate the thermal conductivity depth profile and use only few layers. The fewer the number of layers, the less the ill-posedness of the inverse problem is, yet losing spatial resolution in the reconstruction.⁷ Under these conditions a regular least-square fitting procedure is used to retrieve the few unknowns. However, as the number of layers used in the model is increased, in order to improve the spatial resolution

of the conductivity depth profile, the problem becomes severe ill-posed and more elaborated inversion procedures need to be used⁸ like stabilized least-square fitting,^{4,5} neural networks,^{9,10} and genetic algorithms.¹¹

The aim of this work is to elaborate an inverse algorithm to obtain a thermal conductivity depth profile in case hardened steel plates combining a high in-depth spatial resolution and a high accuracy. To do this we propose an inverse algorithm based on an advanced least-square fitting of the surface temperature including the following improvements: (a) a new normalization procedure to avoid the effect of the different surface qualities of the hardened and unhardened samples, since both kind of samples exhibit different absorption coefficient and infrared emissivity, (b) a weighting factor to reduce the contribution of the high frequencies and to increase the one of the low frequencies, (c) the least-square fitting procedure is applied to the amplitude and phase of the surface temperature simultaneously, taking into account the different noise levels of both quantities, (d) a modified Tikhonov regularization procedure is used to stabilize the inversion, and (e) the Morozov discrepancy principle is used as the stopping criterion, i.e., the iterative process is stopped when the residual reaches the noise level.

First we have checked the ability of this improved inverse procedure to reconstruct an exponential thermal conductivity depth profile for which an analytical solution of the surface temperature exists.¹² We have added a uniform white noise to the calculated surface temperature in order to evalu-

^{a)}Electronic mail: agustin.salazar@ehu.es.

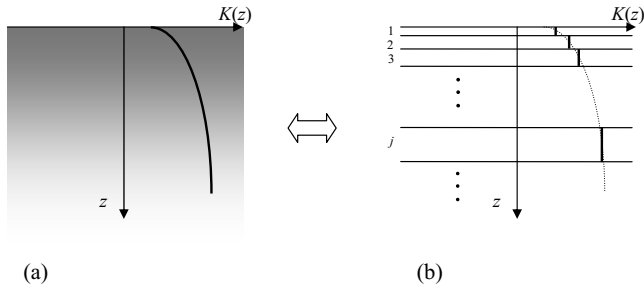


FIG. 1. (a) Scheme of the cross-section of a hardened steel slab showing an in-depth variable thermal conductivity profile. (b) Simulation of the hardened slab by stratified layers, each one having constant thermal conductivity.

ate its influence on the quality of the thermal conductivity reconstruction. Finally, we have used photothermal radiometric measurements performed on several hardened AISI-1018 steel slabs to reconstruct their thermal conductivity depth profile. This profile is in good qualitative anticorrelation with the hardness depth profile, which has been obtained from mechanical indentation tests, confirming the validity of the proposed inversion procedure.

II. INVERSION PROCEDURE

The material we are dealing with is a flat slab of steel whose surface has been hardened after a process of carburizing and quenching. As a consequence, the thermal conductivity is highly reduced at the sample surface, while it remains unchanged inside the slab. The thickness of the surface hardened layer depends on the duration of the heat treatment and usually falls in the range between 0.5 and 2 mm. In this region the thermal conductivity increases almost monotonically as a function of depth [see Fig. 1(a)], the reconstruction of which is the problem at hand. It is worth mentioning that experimental measurements indicate that the heat capacity (ρc), where ρ is density and c specific heat, of the hardened layer remains constant.¹³ In this work, the hardened slab is modeled as an opaque and stratified material [see Fig. 1(b)] made of N parallel layers of thickness l_j , thermal conductivity K_j , and equal heat capacity ρc . In our photothermal experiment the whole surface of the sample is illuminated by a light beam of intensity I_o modulated at a frequency f ($\omega=2\pi f$). We assume that there is no thermal resistance between layers and that heat losses are negligible. The temperature at the illuminated surface can be written in an elegant way using the quadrupole method¹⁴

$$T = \frac{I_o A}{2 C}, \quad (1)$$

where

$$\begin{pmatrix} A & B \\ C & E \end{pmatrix} = \prod_{j=1}^N \begin{pmatrix} A_j & B_j \\ C_j & E_j \end{pmatrix}, \quad (2)$$

being

$$A_j = E_j = \cosh(q_j l_j), \quad B_j = \frac{\sinh(q_j l_j)}{\sqrt{i\omega\rho c K_j}}, \quad \text{and} \quad (3)$$

$$C_j = \sqrt{i\omega\rho c K_j} \sinh(q_j l_j).$$

Here $q_j = \sqrt{i\omega\rho c / K_j}$ is the thermal wave vector. As can be seen, the surface temperature depends on the thermal conductivity and the heat capacity of each layer. It has been demonstrated numerically that the surface temperature of a sample with a continuously variable in-depth thermal conductivity is well reproduced by using a small number of layers (10–20), provided their thickness is not constant, but becomes thinner closer to the surface.¹⁵ According to the multilayer model, we assume that the conductivity $K(z)$ of the hardened slab is a piecewise constant function, with N layers of constant conductivities K_j as the unknowns. To extract information about the thermal conductivity profile of the hardened slab from the experimental temperature we have used a nonlinear least-squares fitting of the experimental data, where we have included the following improvements.

A. Weighting factor

In order to carry out the nonlinear least-square fitting we need to define a norm that measures the differences between the experimental and calculated values of amplitude and phase at all frequencies. In the case where experimental data are taken up to very high frequencies, the regular definition of the norm would diverge due to the big contribution of these high frequencies. For this reason we define a new norm of an arbitrary function F as

$$\|F\| = \int_0^\infty \frac{F^2(f)}{f[\beta + \log^2(f)]} df, \quad (4)$$

that stays finite. Here $\beta = \log^2(f_c)$, f_c being an intermediate frequency in the whole frequency range of the experiment. The denominator in Eq. (4) is the weighting factor introduced (a) for penalizing the contribution of high frequencies, $f \log^2(f)$, and (b) for increasing the relevance of low frequencies, f . Note that β is added to overcome the divergence introduced by the square logarithm at $f=1$ Hz.

B. Normalization procedure

Any experimental set up used to measure the surface temperature introduces a frequency dependence of the system itself, in the experimental data. In order to remove this instrumental factor, the amplitude and phase of the hardened material are always normalized to the data corresponding to an unhardened sample. However, the hardened and unhardened samples exhibit different surface qualities, i.e., different absorption coefficient to the illumination and different infrared emissivity. For this reason, the normalized amplitude is affected by an unknown factor and the normalized phase by an unknown shift. Some authors introduce these quantities as additional unknowns in the inversion process¹⁶ but this would increase the uncertainty in the parameters we want to retrieve. In this work we propose a renormalization method that removes these constants from the data. In the case of the amplitude this renormalization consists in dividing the amplitude values (A) by the norm as defined in Eq. (4). As far as the phase is concerned the renormalization consists in subtracting the mean value of all the phase values

$$A_N(f) = \frac{A(f)}{\|A\|}, \quad (5a)$$

$$\psi_N(f) = \psi(f) - \langle \psi \rangle, \quad (5b)$$

where

$$\langle \psi \rangle = \frac{\int_0^\infty \frac{\psi}{f[\beta + \log^2 f]} df}{\int_0^\infty \frac{1}{f[\beta + \log^2 f]} df}. \quad (6)$$

Note that the renormalized amplitude and phase are invariant under expansion of the amplitude and phase shifts, i.e., the unknown constants affecting both the normalized amplitude and the normalized phase have been removed.

C. Simultaneous fitting of amplitude and phase

Among the different inversion procedures proposed in the literature (neural networks, genetic algorithms, etc) we have selected the nonlinear least-square fitting of the experimental data implemented by several improvements. The ordinary least-square fitting consists in finding the conductivity parameters of each layer which minimize the residual function defined as $\int_0^\infty F^2(f)df$, where F is the difference between the experimental and calculated temperatures. It has been pointed out that the experimental values of the amplitude and phase of the surface temperature must be fitted simultaneously to retrieve a unique thermal conductivity profile.¹⁷ Our first attempts did not give meaningful conductivity reconstructions mainly due to the different noise of amplitude and phase. Therefore, we decided to minimize a single function containing the renormalized amplitude and phase, and including a balance factor of their noises.

We define the noise level as the norm [see Eq. (4)] of the difference between noisy and noise-free data at each frequency. As the noise-free data are unattainable, we estimate this difference as the half-value of the thickness of the “data cloud” (ε_A for amplitude and ε_ψ for phase). Then the noise-levels (δ_A and δ_ψ) are given by the norm of two “noise-vectors” whose n entries (n is the number of frequencies) are random values between $+\varepsilon_A$ and $-\varepsilon_A$ for amplitude, and $+\varepsilon_\psi$ and $-\varepsilon_\psi$ for phase. Accordingly, the residual function to be minimized is

$$\begin{aligned} r(K) &= \int_0^\infty \frac{[A_{N_{\text{the}}}(f) - A_{N_{\text{exp}}}(f)]^2}{f[\beta + \log^2(f)]} df \\ &+ \gamma^2 \int_0^\infty \frac{[\psi_{N_{\text{the}}}(f) - \psi_{N_{\text{exp}}}(f)]^2}{f[\beta + \log^2(f)]} df \\ &= \int_{-\infty}^\infty \frac{[A_{N_{\text{the}}}(u) - A_{N_{\text{exp}}}(u)]^2}{\beta + u^2} du \\ &+ \gamma^2 \int_{-\infty}^\infty \frac{[\psi_{N_{\text{the}}}(u) - \psi_{N_{\text{exp}}}(u)]^2}{\beta + u^2} du, \end{aligned} \quad (7)$$

where $u = \log(f)$ and the factor $\gamma = \delta_A / \delta_\psi$ is introduced to balance the noise levels of the two quantities that we are com-

paring for the minimization, i.e., we introduce this factor in order to reduce the contribution of the quantity that has a larger error. The noise level of the experiments is then: $\delta = \sqrt{\delta_A^2 + \gamma^2 \delta_\psi^2} = \delta_A \sqrt{2}$.

D. Regularization procedure

As we intend to use a large number of layers in order to reach a high spatial resolution in K reconstruction we need to deal with a large number of unknowns which turns the inverse problem severe ill-posed. Accordingly, the regular least-square fitting rule will lead to unstable (oscillating) iterations related to the existence of an undetermined number of minima. In order to overcome these instabilities researchers have used different approaches: the conjugate gradient method, the single value decomposition approach, the nonlinear Landweber iteration, among others.^{8,18} In this work we have used the Tikhonov's regularization procedure which consists in adding a stabilization term to the residual function r , followed by an iterative Newton-type method of minimization.

As we are using the quadrupole method for solving the direct problem, our calculated amplitude and phase are functions of N conductivities, one for each layer. On the other hand, our data correspond to discrete values of the frequency. Therefore, the function to be minimized is the discretization of Eq. (7) including the regularization term and writes

$$\begin{aligned} r_\alpha(K_1, \dots, K_N) &= \alpha J(K_1, \dots, K_N, K_1^0, \dots, K_N^0) \\ &+ \sum_{i=1}^M \frac{[A_{N_{\text{the}}}(K_1, \dots, K_N, u_i) - A_{N_{\text{exp}}}(u_i)]^2}{\beta + u_i^2} \Delta u_i \\ &+ \gamma^2 \sum_{i=1}^M \frac{[\psi_{N_{\text{the}}}(K_1, \dots, K_N, u_i) - \psi_{N_{\text{exp}}}(u_i)]^2}{\beta + u_i^2} \Delta u_i, \end{aligned} \quad (8)$$

where K_j are the values of the conductivities of each layer and M the number of frequencies of the experiment. As the experimental frequencies are usually taken equally spaced in a logarithmic scale, Δu_i is constant, and therefore r_α writes in a simple form very suitable for practical purposes. The second and third terms of the right-hand side are the discrete version of the residual, r , and the first term is the Tikhonov penalty term,¹⁸ being $\alpha > 0$ the regularization parameter and K_j^0 with $j = 1, \dots, N$ an initial guess of the conductivities. In addition to stabilizing the minimization, this term has the advantage of being able to incorporate prior information about the problem, e.g., in hardened materials $K_N^0 = K_{\text{unhardened}}$. Here J is the penalty function. The standard Tikhonov penalty function is $J(K_1, \dots, K_N, K_1^0, \dots, K_N^0) = \sum_{j=1}^N I_j(K_j - K_j^0)^2$. However, in order to reduce the number of iterations to achieve the minimum, we have used a modification of the standard penalty function

$$\begin{aligned}
& J(K_1, \dots, K_N, K_1^0, \dots, K_N^0) \\
&= \sum_{j=1}^{N-1} \frac{1}{l_j} [(K_{j+1} - K_j) - (K_{j+1}^0 - K_j^0)]^2 \\
&+ \frac{1}{l_N} (K_{\text{unhardened}} - K_N)^2. \tag{9}
\end{aligned}$$

Note that with the standard penalty function the conductivities of the layers are kept close to the initial guess, while in the modified function, both the derivatives of the conductivity together with the conductivity of the deepest layer are kept close to the corresponding initial guess values.

The iterative algorithm that we have used to minimize the function r_α in Eq. (8) is a Newton-type method which consists in a variant of the iterative Levenberg–Marquardt method, suggested by Bakushinskii,¹⁹ that allows incorporating the Tikhonov’s penalty term. Briefly speaking, in each iteration a reconstruction of the thermal conductivity $K(z)$ is retrieved by solving a linear system of equations, using continuously decreasing α values according to $\alpha_{n+1} = \eta \alpha_n$ with $\eta \in (0, 1)$. The reduction factor η governs the rate of convergence: the lower the η value, the faster the rate. However, there is not a general rule to choose its best value since a very small η value reduces the stabilization introduced by the Tikhonov’s penalty term. In this work we have used η in the range from 0.4 to 0.8.

E. Stopping criterion

It should be noted that although the penalty term stabilizes the minimization process it also adds an additional error to the model. Therefore, the question is the suitable choice of the regularization parameter α that guarantees stability (high α) with the lowest additional error (low α). We will make this selection as a function of the noise level of the experimental data by using the Morozov discrepancy principle.²⁰ We stop the iterations the first time the residual [the second and third terms in the right hand of Eq. (8)] reaches the noise level δ .

The need for stopping the iterations is the following. In the iterative process the residual function is reduced while the reconstructed thermal conductivity approaches the real value. However, due to the noise of the experimental data, the effect of keeping on with the iterations is that, although the value of the residual function still diminishes, the reconstructed conductivity becomes nonsense. The reason for this is that the fitting procedure tries to reproduce the experimental data, which are affected by the noise (overfitting). Summarizing, for each set of experimental data there is a number of iterations giving the best K reconstruction. Looking for an automatic iterative process we need to define a stopping criterion based on the experimental noise, as the Morozov discrepancy principle.

III. NUMERICAL CALCULATIONS

In this section we present some results using synthetic data in order to show the improvements in the reconstruction introduced by the method we have developed. We used analytically calculated values of the amplitude and phase of the

surface temperature as a function of the modulation frequency of a semi-infinite slab whose conductivity decreases exponentially in depth.¹² It is worth mentioning that analytical solutions are used in order to avoid “inverse crimes,” i.e., an excessively optimistic inversions that occurs when the same numerical methods are employed to synthesize as well as to invert data in an inverse problem.²¹ Our theoretical experiments consist in generating noisy data by adding uniform white noise to the calculated amplitudes and phases and retrieving the (known) conductivity depth profile. In this way, for these “theoretical experiments,” we can evaluate the uncertainty in the recovered conductivity.

In order to retrieve a conductivity profile, we need to determine the number and thicknesses of the layers that will be used for the reconstruction. We use an exponentially increasing sequence of layer thicknesses. The number of layers is determined as a function of the uniform white noise we add in our synthetic data, since the error introduced by our discrete and finite layer model cannot be larger than the “experimental” random noise we are simulating. Accordingly, the lower the experimental noise, the larger the number of layers used for the reconstruction must be. In practice we choose the width of the shallower layer as a function of the random noise. Assuming a certain penetration depth and an exponential law for the layer thicknesses, the thicknesses of all layers are determined.

The synthetic data we generate correspond to a discrete set of frequencies ranging from f_{\min} to f_{\max} , equally spaced in a logarithmic scale. For the sake of simplicity, we use the same number of layers and frequencies, the lower frequency being determined by the hardening penetration depth and the higher one limited by the error. Note that, given a certain noise level in a real experiment, this criterion for the choice of frequencies with synthetic data can also be used to determine the optimum set of frequencies at which experimental data should be taken.

Now we show the effect of the frequency weighting in the quality of the reconstructed conductivity profile. For this purpose, we have generated synthetic data by adding to the analytically calculated amplitude and phase uniform white noise of the same order as the noise in our experimental data (random noise vectors of amplitude $\varepsilon_A = \pm 0.025$ for temperature amplitude and $\varepsilon_\psi = \pm 0.5^\circ$ for the phase). We have used frequencies from 5×10^{-1} up to 10^4 Hz, the same range of our experiments. We assume that the heat capacity remains constant, $\rho c = 3 \times 10^6$ J m⁻³ K⁻¹, and we fit the data down to 1 mm in depth. In Fig. 2 we show, on top, the exponentially decreasing conductivity profile (solid line), given by $K(z) = 50 \exp(-10^3 z)$ W m⁻¹ K⁻¹, that we have used to calculate the surface temperature amplitude and phase, together with the reconstructed conductivities at the first seven iterations (in symbols). On the left we show the reconstruction using frequency weighting while the reconstruction without frequency weighting is depicted on the right. The open symbols correspond to the iteration at which the Morozov criterion stops the iterative process (fifth iteration in both cases). At the bottom, in dots we show the value of the residual r at each iteration together with the noise level δ of the experiment, which determines the Morozov stopping

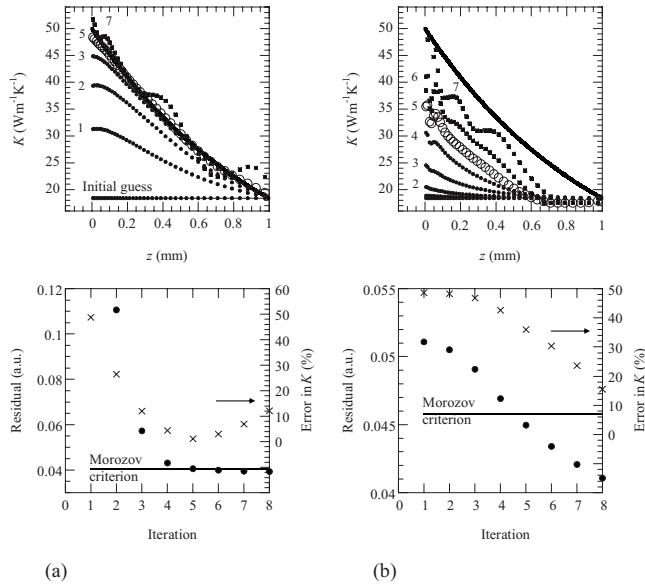


FIG. 2. On top, the true theoretical exponentially decreasing conductivity profile (solid line), and reconstructed conductivities for the first seven iterations (in symbols). Inversion has been performed from amplitude and phase data generated in the frequency range 10^{-1} – 10^4 Hz, with random noise $\varepsilon_A = \pm 0.025$ and $\varepsilon_\psi = \pm 0.5^\circ$. At the bottom, in crosses, the error in the conductivity at each iteration, together with the residual (in dots), and the Morozov stopping criterion (solid line). (a) Reconstructions using frequency weighting and (b) reconstructions without frequency weighting.

criterion (solid line). In crosses, we represent the relative error in the conductivity at each iteration. In both cases, the initial guess is a constant conductivity profile corresponding to the conductivity at $z=1$ mm.

As can be observed, if no frequency weighting factor is introduced, the conductivity profile cannot be reconstructed. The reason for this is that since the temperature data correspond to the surface of the sample, the high frequencies containing information from positions close to the surface dominate the reconstruction. The information coming from deeper inside the material, contained in the low frequencies, becomes completely masked. This is revealed in the fact that the successive reconstructed conductivities differ from the initial guess only at the closest layers to the surface (only down to 0.65 mm at the fifth iteration). On the opposite, the reconstruction is very good when we introduce the frequency weighting factor, which balances the contributions of high and low frequencies in the fitting process.

The first iteration at which the residual is smaller than the noise level (continuous horizontal line) gives the final result in the automatic process. Note that, although the data to be fitted are the same in both cases, the noise level δ (Morozov criterion) is different because it is calculated according to the presence (or absence) of the weighting factor. However, in order to illustrate the importance and the effect of the stopping criterion, we show the results of a few more iterations. In both cases, with and without frequency weighting, the residual diminishes with the number of iterations, but the error in the thermal conductivity increases at certain iteration after the Morozov criterion stops the iterative process. This corresponds to the above mentioned overfitting. The conductivity reconstructions corresponding to iterations

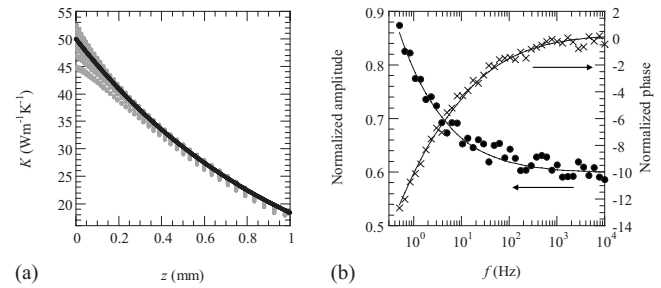


FIG. 3. (a) The true exponentially decreasing conductivity profile (solid line) together with the reconstructions obtained starting at ten different linear initial guesses (in dots). For each initial guess we fit two data sets, affected by different white noise vectors, both corresponding to $\varepsilon_A = \pm 0.025$ and $\varepsilon_\psi = \pm 0.5^\circ$, in the frequency range 5×10^{-1} – 10^4 Hz. (b) Synthetic amplitude (dots) and phase (crosses) data corresponding to the exponential conductivity profile depicted in (a), together with the best fittings (continuous lines).

7 and successive show an oscillating behavior with no physical meaning. These oscillations are the result of minimizing function r_α in Eq. (8) with a Tikhonov term which has been reduced to such a point that it does not stabilize the process anymore.

The Morozov criterion guarantees that the retrieved conductivity is meaningful at the price of a reconstructed profile that does not correspond to the best possible (minimum error of the conductivity). However, in a real experiment, the “true” conductivity profile is unknown and the priority is to find a meaningful reconstruction.

Next, we show how the noise in the amplitude and phase data affects the reconstructed conductivity. To do so, we have proceeded as follows: for the same exponentially decreasing conductivity profile [solid line in Fig. 3(a)] we start the reconstruction at ten different linear initial guesses. These are characterized by a common conductivity value at 1 mm depth ($50/e$ $\text{W m}^{-1} \text{K}^{-1}$) and surface conductivities of values 75, 70, 65, 60, 55, 50, 45, 40, 35, and 30 $\text{W m}^{-1} \text{K}^{-1}$. For each initial guess we fit amplitude and phase synthetic data generated with two sets of random noise vectors. In Fig. 3(a), we show the true conductivity (solid line) together with all the 20 retrieved conductivity profiles (symbols). Figure 3(b) shows amplitude (dots) and phase (crosses) synthetic data used for the fittings (solid lines) that we have generated from the exponentially decreasing conductivity profile by adding the same white noise as in Fig. 2. These fittings correspond to the linear initial guess with conductivity 65 $\text{W m}^{-1} \text{K}^{-1}$ at the surface, but indistinguishable fittings were obtained starting at all the different initial guesses. We have slightly overestimated the Morozov level in order to prevent oscillations to occur in the reconstructed conductivity. Figure 4(a) shows the same calculations but starting from synthetic data generated with the previous noise level divided by 4. As can be observed, as the error in the data decreases, the dispersion in the reconstructed conductivity is reduced and the mean value of the conductivities at each layer approaches the real conductivity. This is a fundamental characteristic of a good inversion method: the result given by the method should approach the true profile when the error in the data tends to zero.

Finally, we show the effect of reducing the frequency

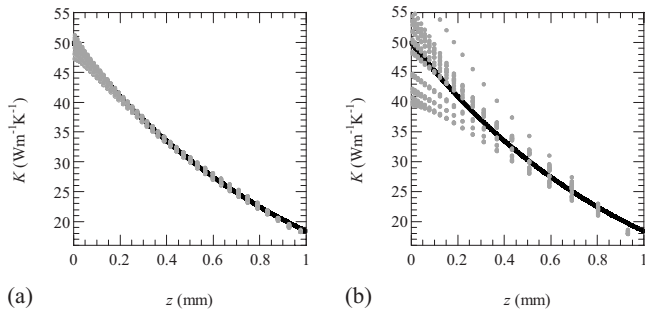


FIG. 4. (a) The same as in Fig. 3(a), but with the noise reduced by a factor of 4. (b) The same as in Fig. 3(a) but with amplitude and phase data fitted in a narrower frequency range: $5 \times 10^{-1} - 10^2$ Hz.

range in which amplitude and phase data are fitted. If we perform the same calculations as above, with white noise like in Fig. 3(a) but taking data only up to 10^2 Hz instead of 10^4 Hz, we obtain the reconstructions depicted in Fig. 4(b). Suppression of high frequencies results in a bigger dispersion of the retrieved conductivities, mainly in the shallower layers. The reason for this is the following: as the true conductivity profile is varying close to the surface, high frequencies contain relevant information in order to reconstruct the conductivity profile close to the surface.

IV. EXPERIMENTAL RESULTS

Now we will use the method described above to retrieve the thermal conductivity profile of a semi-infinite AISI 1018 sample, which has been hardened to a nominal case penetration depth of the order of 1 mm.²² Fig. 5(a) shows the normalized amplitude (dots) and phase (crosses) of the surface temperature measured with a photothermal radiometry setup, corresponding to 51 frequencies equally spaced in a logarithmic scale. We have used the same number of layers for the reconstruction. In order to fulfill the one-dimensional heat propagation, the exciting beam was expanded to a radius of 20 mm, which is much larger than the thermal diffusion length in the sample at the lowest modulation frequency [$\mu = \sqrt{D/(\pi f)} \approx 3$ mm at 0.5 Hz].

As the nominal case penetration depth is close to 1 mm, we have performed several conductivity reconstructions assuming different penetrations depths in the range from 0.9 to 1.7 mm. In all reconstructions the same initial guess $K_j^0 = K_{\text{unhardened}}$ has been used. On the other hand, as mentioned

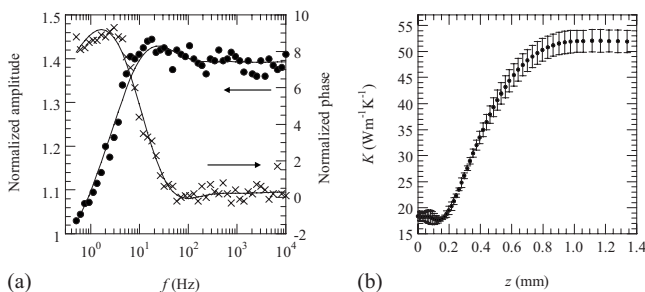


FIG. 5. (a) Experimental amplitude (dots) and phase (crosses) data corresponding to a hardened AISI 1018 steel flat semi-infinite sample, together with the fittings (solid lines). (b) Thermal conductivity reconstruction from the data depicted in (a).

in Sec. II C, the calculation of the noise level δ determining the stopping criterion requires generating two noise vectors with random entries between $\pm \varepsilon_A$ for amplitude and $\pm \alpha_\psi$ for the phase, and the calculation of their norms. It is worth noting that this estimation of the noise level should never be smaller than the real noise, otherwise, the stopping criterion would never be reached. Of course, the value of the resulting noise level δ , depends on the particular set of random entries of the noise vectors, and affects the stopping criterion. In order to incorporate the influence of the particular noise vector on the dispersion of the reconstruction, we generate five different noise vectors for each penetration depth, all with random entries between $\pm \varepsilon_A = 0.025$ (amplitude) and $\pm \varepsilon_\psi = 0.5^\circ$ (phase), given by the data cloud of the experimental data. In the corresponding 40 reconstructions, the Morozov level moves as much as 50%; and therefore, its influence becomes the most relevant source of uncertainty in the reconstructed profiles.

In Fig. 5(b), we show the mean conductivity obtained at each depth together with error bars corresponding to the standard deviation of the 40 reconstructed conductivities. Several aspects deserve comment in this figure: (a) the error in the conductivity is about 4% all along the hardened depth. The result reveals the relevance of introducing the frequency weighting which results in a conductivity error which does not increase as we go deeper inside the material. The reason for this error to be rather small is that prior information is available in our problem and we are able to incorporate it in our penalty term. (b) The reconstructed conductivity is almost flat at locations close to the surface (down to 150 μm). (c) Moreover, this retrieved conductivity profile is in good qualitative anticorrelation with the hardness depth profile (see Fig. 9 in Ref. 22), in agreement with previously reported results.^{13,23} (d) The amplitude and phase fittings barely differ from one reconstruction to another. As an example, the solid line in Fig. 5(b) shows the fitted amplitude and phase corresponding to one of the reconstructions. The asymptotic behavior we observe in the experimental amplitude and phase at high frequencies is related to the fact that the conductivity profile is almost flat close to the surface.

The usefulness of taking data up to very high frequencies deserves some discussion. High frequency data contain information about shallow locations and, thus, the determination of the conductivity at these positions is an easier question than determining the conductivity of the deeper layers. As we have shown in Figs. 3(a) and 4(b), if the true conductivity is changing close to the surface, the information contained in the high frequencies is relevant to properly reconstruct the conductivity profile close to the surface. In the case of hardening, where quasiflat conductivity profiles close to the surface have been reported in the literature in several works,^{17,24} high frequencies are not so important for determining the shape of the profile close to the surface. Moreover, if high frequency data are noisy, the uncertainty in the surface conductivity will be high, which makes the high frequency data useless. This is why the effort of taking data at very high frequencies is only worth in the case that low experimental noise can be achieved.

V. CONCLUSIONS

The problem of retrieving a thermal conductivity profile from surface temperature data has been successfully solved by performing the direct temperature calculation using the quadrupole method and by applying an inversion procedure based on a stabilized least square fitting method, where we have introduced several improvements. The effect of these improvements has been analyzed by retrieving conductivity profiles from noisy synthetic data generated from a known conductivity profile. First, we have proceeded to perform a renormalization of the experimental data in order to eliminate experimental constants affecting both the amplitude and the phase. Thanks to this renormalization, these constants that appear as additional unknowns in the problem of retrieving the conductivity profile, are removed. Second, we have combined the amplitude and phase data for the minimization and have balanced both according to the noise they exhibit. This allows us to penalize the magnitude with the bigger noise i.e., we increase the significance of the magnitude with less uncertainty in the inversion. Moreover, the introduction of a frequency weighting factor penalizing the influence of the high frequencies and increasing that of the low frequencies allows getting a realistic reconstructed profile that we were unable to obtain without using the frequency weighting factor. The ill-posed character of the inverse problem requires the use of regularization term in the minimization of the residual. We have chosen a modification of the Thikonov penalty term, and have used the Morozov discrepancy principle to stop the iterations. We have analyzed the influence of using this stopping criterion on the quality of the reconstructed conductivity, by studying the effect of the noise and the frequency range on the final reconstruction. According to these conclusions, we have retrieved a thermal conductivity profile from experimental data obtained from a stainless steel hardened sample, with a very low dispersion even at deep locations, and in good qualitative anticorrelation with the results of a hardening indentation test.

ACKNOWLEDGMENTS

This work has been supported by the Ministerio de Educación y Ciencia through research Grant No. MAT2008-01454, by the Universidad del País Vasco through research Grant No. DIPE08/10, and by the Diputación General de Aragón.

- ¹M. Munidasa, M. Tian-Chi, A. Mandelis, S. K. Brown, and L. Mannik, *Mater. Sci. Eng., A* **159**, 111 (1992).
- ²A. Mandelis, F. Funak, and M. Munidasa, *J. Appl. Phys.* **80**, 5570 (1996).
- ³J. Fizez and J. Thoen, *J. Appl. Phys.* **75**, 7696 (1994).
- ⁴T. N. Lan, U. Siedel, and H. G. Walther, *J. Appl. Phys.* **77**, 4739 (1995).
- ⁵C. Glorieux, J. Fizez, and J. Thoen, *J. Appl. Phys.* **73**, 684 (1993).
- ⁶A. Mandelis, S. B. Peralta, and J. Thoen, *J. Appl. Phys.* **70**, 1761 (1991).
- ⁷C. Wang, A. Mandelis, and Y. Liu, *J. Appl. Phys.* **97**, 014911 (2005).
- ⁸M. N. Özisik and H. R. B. Orlande, *Inverse Heat Transfer: Fundamentals and Applications* (Taylor & Francis, New York, 2000).
- ⁹C. Glorieux, R. Li Voti, J. Thoen, M. Bertolotti, and C. Sibilía, *Inverse Probl.* **15**, 1149 (1999).
- ¹⁰C. Glorieux and J. Thoen, *J. Appl. Phys.* **80**, 6510 (1996).
- ¹¹R. Li Voti, C. Sibilía, and M. Bertolotti, *Int. J. Thermophys.* **26**, 1833 (2005).
- ¹²J. Fizez and J. Thoen, *J. Appl. Phys.* **79**, 2225 (1996).
- ¹³H. G. Walther, D. Fournier, J. C. Krapez, M. Luukkala, B. Schmitz, C. Sibilía, H. Stamm, and J. Thoen, *Anal. Sci.* **17**, s165 (2001).
- ¹⁴D. Maillat, S. André, J. C. Batsale, A. Degiovanni, and C. Moyne, *Thermal Quadrupoles* (Wiley, New York, 2000).
- ¹⁵R. Celorrio, A. Mendioroz, E. Apiñaniz, A. Salazar, C. Wang, and A. Mandelis, *J. Appl. Phys.* **105**, 083517 (2009).
- ¹⁶L. Nicolaidis, A. Mandelis, and C. J. Beingsner, *J. Appl. Phys.* **89**, 7879 (2001).
- ¹⁷J. Fizez and J. Thoen, *J. Appl. Phys.* **81**, 2963 (1997).
- ¹⁸H. W. Engl, M. Hanke, and A. Neubauer, *Regularization of Inverse Problems* (Kluwer Academic, Dordrecht, 2000).
- ¹⁹A. B. Bakushinskii, *Comput. Math. Math. Phys.* **32**, 1353 (1993).
- ²⁰T. Bonesky, *Inverse Probl.* **25**, 015015 (2009).
- ²¹D. Colton and R. Kress, *Inverse Acoustic and Electromagnetic Scattering Theory* (Springer, Berlin, 1998), p. 133.
- ²²C. Wang, A. Mandelis, H. Qu, and Z. Chen, *J. Appl. Phys.* **103**, 043510 (2008).
- ²³T. N. Lan, U. Siedel, H. G. Walther, G. Goch, and B. Schmitz, *J. Appl. Phys.* **78**, 4108 (1995).
- ²⁴M. Munidasa, F. Funak, and A. Mandelis, *J. Appl. Phys.* **83**, 3495 (1998).